

Mechanical properties of carbynes investigated by *ab initio* total-energy calculations

Ivano E. Castelli,¹ Paolo Salvestrini,² and Nicola Manini³

¹*Center for Atomic-scale Materials Design, Department of Physics, Technical University of Denmark, DK-2800 Kongens Lyngby, Denmark*

²*CNR-IFN - Istituto di Fotonica e Nanotecnologie,*

Sezione di Milano, Piazza L. Da Vinci 32, 20133 Milano, Italy

³*ETSF and Dipartimento di Fisica, Università degli Studi di Milano, Via Celoria 16, 20133 Milano, Italy*

As *sp* carbon chains (carbynes) are relatively rigid molecular objects, can we exploit them as construction elements in nanomechanics? To answer this question, we investigate their remarkable mechanical properties by *ab-initio* total-energy simulations. In particular, we evaluate their linear response to small longitudinal and bending deformations and their failure limits for longitudinal compression and elongation.

PACS numbers: 62.25.-g, 81.07.Gf, 62.20.de, 46.70.De

I. INTRODUCTION

The rich chemistry of carbon is due to the capability of its electronic configuration to adjust to different bonding situation. Carbon atoms realize three main hybridization schemes of the valence orbitals: *sp*³, *sp*², and *sp* hybridization. *sp*³ bonding tends to form three-dimensional networks, as in diamond and the related amorphous structures. *sp*²-hybridized orbitals lead to two-dimensional networks, at the basis of graphene, graphite, fullerenes, nanotubes, ribbon structures, and other forms of wide current interest for their unique mechanical and electronic properties. *sp*-hybridized carbon forms linear structures (carbynes), which, compared to their chemically more stable *sp*³ (alkanes) and *sp*² (alkenes) hydrogenated counterparts, tend to be rigid, thus potentially appealing as backbones for molecular nanotechnology.

Carbynes of increasing length and varied terminations are being synthesized^{1–4} and characterized.⁵ At the same time, the fabrication of carbon atomic chains from stretched nanotubes or graphene was achieved by controlled electron irradiation in transmission electron microscopes.^{6–8} The remarkable robustness of these carbon chains under irradiation combined with the ease of electron-beam fabrication at the nm scale can provide a route to the synthesis of actual nano-devices based on carbynes. Recent investigations have elucidated the prominent role of molecular oxygen as a primary source of chemical degradation of *sp* carbon^{9,10}. In a pure-carbon environment carbynes are far more stable^{11–15}.

Effects of longitudinal straining^{16–19} and lateral bending²⁰ were investigated very recently by *ab-initio* methods. The outcome of those studies is that carbyne chains are at one time extremely stiff against longitudinal straining and very soft against a bending deformation, to the extent that even extreme bending affects only moderately their bonding properties.²⁰ In the present paper we focus on the mechanical properties of carbynes in the perspective of exploiting them as construction materials for nano-engineering. We use *ab-initio* simulations^{13,21}

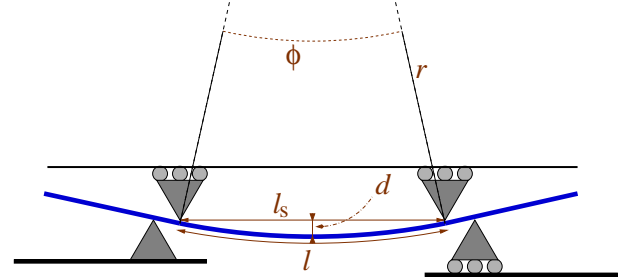


FIG. 1: (Color online) A beam model used to describe the mechanical properties of a *sp*-carbon chain subject to straining. The scheme represents the relaxed configuration of the beam subjected to four lateral constraints, which induce two bending moments on the beam central section, which, as a result, bends as the arc of a circle. We identify the end-to-end distance l_s of the deformed region; the curvilinear beam length l ; the maximum deflection d from straight geometry; the radius of curvature r ; and the deflection angle ϕ .

to predict the stiffness of the carbynes for both longitudinal strain and for bending, and their ultimate tensile strength. The main results of these simulations is that a *sp* carbon chain (and it matters little whether it is of cumulenic – all double bonds, or polyynic – with alternating single-triple bonds) exhibits not only an exceptional mechanical stiffness against longitudinal deformations, but also a small but nonzero rigidity against bending. Accordingly, a C_n chain resembles a thin beam characterized by a finite rigidity against buckling, rather than a string. We find that, e.g., a single-carbyne C_8 “pillar” can withstand a modest but non-negligible axial compression force ~ 0.7 nN before buckling.

II. THE MODEL

In simulations, one can tune the carbyne length by fixing the position of the end carbon atoms of a selected chain section, and leave all other atoms free to relax to their equilibrium position, compatible with the imposed

strain. As well known to civil engineers, as soon as the compressive stress exceeds a critical value, the straight configuration of a beam subject to a purely axial strain $\varepsilon < 0$ turns unstable and “buckles” spontaneously to a curved arc. In the simulations of highly strained configurations, it is straightforward to address either the metastable straight configuration, or the stable buckled configuration investigated in Ref. 20.

To characterize the mechanical properties of a carbyne segment, and in particular to evaluate the buckling transition, one needs to identify the correct linear-response parameters in a simple model where the effects of different kinds of deformations can be decoupled and studied separately. The simplest continuum model describes a carbyne as a strained thin beam of a homogeneous material, thereby ignoring its discrete atomic structure. Three basic deformations can be applied to the beam: longitudinal traction or compression; lateral bending, as sketched in Fig. 1; torsion around its axis. Correspondingly, the elastic deformation energy can be decomposed as:

$$E_{\text{el}} = E_{\text{tens}} + E_{\text{bend}} + E_{\text{tors}}, \quad (1)$$

where E_{tens} is the tensile energy increase due to longitudinal elongation/shortening, E_{bend} is the energy due to the pure flexion of the beam, and E_{tors} is the energy increase due to the twisting of the beam. Remarkably, even this third term is important for the essentially 1D cumulenes.¹³ In the present work we will however mostly ignore torsion, and concentrate on the first two terms.

In the linear-response (small-strain) regime, we write the tensile energy in terms of the strained length l relative to the fully relaxed length l_0 as

$$E_{\text{tens}} = \frac{1}{2} \frac{\chi}{l_0} (l - l_0)^2, \quad (2)$$

where χ/l_0 is the elastic stiffness of the beam, and χ is the length-independent beam elastic tension: in the continuum mechanics of 3D solids $\chi = \mathcal{E} \cdot A$, the product of the material’s elasticity modulus times the beam transverse area.

Figure 1 indicates the relevant geometrical quantities characterizing the pure-bending deformations of a carbyne of fully relaxed length l_0 . In a circular-arc geometry ensuing from the application of a small bending moment M at the beam ends, the bending energy can be derived by the linear relation of the deflection angle ϕ with the applied bending moment:

$$\phi = \frac{Ml}{g}, \quad (3)$$

Here g is the length-independent bending stiffness of the beam: in 3D continuum mechanics $g = E \cdot I$, the product of the elasticity modulus times the second moment of area of the beam cross section. (The dimension of g is force \times area.) For a circular deformation, the bending energy E_{bend} is therefore

$$E_{\text{bend}} = \frac{1}{2} M\phi = g \frac{\phi^2}{2l}. \quad (4)$$

It is convenient to express all quantities in terms of clearly defined geometrical quantities, e.g. the distance l_s between the end points of the chain and the maximum deflection d from straight geometry. We have:

$$\phi = 4 \arctan \frac{2d}{l_s} \quad (5)$$

$$l = \phi r = \frac{\phi}{2 \sin \frac{\phi}{2}} l_s. \quad (6)$$

With the implicit substitution of the expressions (5) and (6), the elastic energy of the beam stretched and/or bent in a circular arc is therefore

$$E_{\text{mech}} = E_{\text{tens}} + E_{\text{bend}} = \frac{1}{2} \frac{\chi}{l_0} (l - l_0)^2 + g \frac{\phi^2}{2l}. \quad (7)$$

III. CALCULATIONS

We determine the linear-response parameters χ and g by means of simulations based on the density functional theory (DFT) in the local density approximation (LDA). The time-honored LDA is one in many functionals being used for current DFT studies of molecular systems: other functionals often improve one or another of the systematic defects of LDA (underestimation of the energy gap, small overbinding and overestimation of the vibrational frequencies), but to date no functional is universally accepted to provide systematically better accuracy than LDA for all properties of arbitrary systems. For a covalent system of s and p electrons as the one studied here, LDA is appropriate, and we expect our results to change by a few percent at most if the calculations were repeated using some other popular functional.^{22–24}

We compute the total adiabatic energies by means of the plane-waves DFT code Quantum Espresso.^{25–39} We consider the two different limiting structures of carbynes: polyynes (or α -carbynes) with alternating single–triple bonds ($\dots - \text{C} \equiv \text{C} - \text{C} \equiv \text{C} - \dots$), contrasted to cumulenes or β -carbynes, with nearly-equal-length (double) bonds ($\dots = \text{C} = \text{C} = \dots$). A typical polyyne chain is obtained when each end carbon atom forms a single bond with a ligand (e.g. a hydrogen atom, as in diacetylene), while a typical cumulene is obtained when each end carbon forms a double bond, for example to a CH_2 group, as in ethylene.

We focus on a C_8 chain segment, and compare its mechanical response in its $\text{HC}_2\text{-C}_8\text{-C}_2\text{H}$ polyyne and $\text{H}_2\text{C-C}_8\text{-CH}_2$ cumulenic realizations. For the polyyne, we select hydrogenacetylide terminations rather than a single hydrogen because the $\text{HC}_2\text{-}$ group allows us to impose a bending moment at the ends of the C_8 chain as in Fig. 1, by displacing a C atom along the chain continuation rather, than a chemically different H atom, thereby probing the intrinsic properties of carbyne, rather than those of a specifically-terminated compound. We also consider C_n polyyne of different lengths, to check for size effects, and a 90° end-twisted C_8 cumulene, which

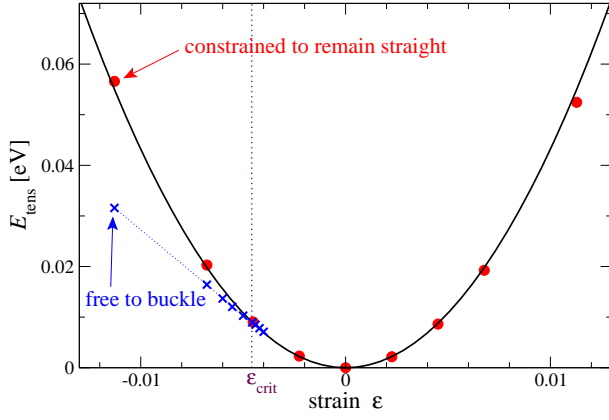


FIG. 2: (Color online) The DFT-LDA tensile excess energy computed for the strained straight $\text{HC}_2\text{-C}_8\text{-C}_2\text{H}$ polyynic (bullets), as a function of $\varepsilon = (l - l_0)/l_0$. Solid line: a quadratic fit of Eq. (2), restricted to the 7 data points within $\pm 0.8\%$ strain, where deviations from the linear-response regime are negligible. Crosses: the total excess energy without the constraint that the chain should remain straight: buckling starts to build up for strain exceeding $\varepsilon_{\text{crit}}$. The very similar data and fit for the cumulene $\text{H}_2\text{C-C}_8\text{-CH}_2$ is not reported for clarity's sake.

we must treat within the local spin-density approximation (LSDA) since twisting induces a peculiar total spin-1 electronic state, with a twofold-degenerate level occupied by two parallel-spin electrons.¹³ We do not attempt any serious size scaling, for two main reasons: (i) very long carbynes are mechanically unstable (thus unsuitable for nanomechanical applications) anyway, and (ii) the long-range interaction effects demonstrated recently¹⁷ would make a proper *ab-initio* size-scaling determination of the mechanical (in particular bending) properties of long carbynes prohibitively expensive. In the present work we do not deal with the exotic odd- n C_n chains, which are chemically less stable and more difficult to synthesize.^{26,27}

To evaluate χ , starting from the fully relaxed carbyne we stretch or compress a straight C_8 chain section by fixing the positions of the end carbon atoms, and letting all other atoms free to relax to their resulting equilibrium positions under stress. We extract an estimate of χ by fitting Eq. (2) to the resulting values of the excess energy as a function of the chain elongation, as reported in Fig. 2.

To evaluate the bending stiffness g , we force the chain to bend by imposing a small lateral displacement of the two atoms adjacent to the C_8 section of the chain, while keeping the first and last atom in the chain section bounded to remain laterally undispaced, following the scheme of Figs. 1 and 3 (inset). We then let all other degrees of freedom (including the axial position of the laterally bounded atoms) of the chain relax. The C_8 section relaxes to form a circular arc, which we fit⁴⁰ to extract the geometrical quantities indicated in Fig. 1. Note that this procedure differs substantially from the fixed-end approach of Ref. 20, where longitudinal and bending strains

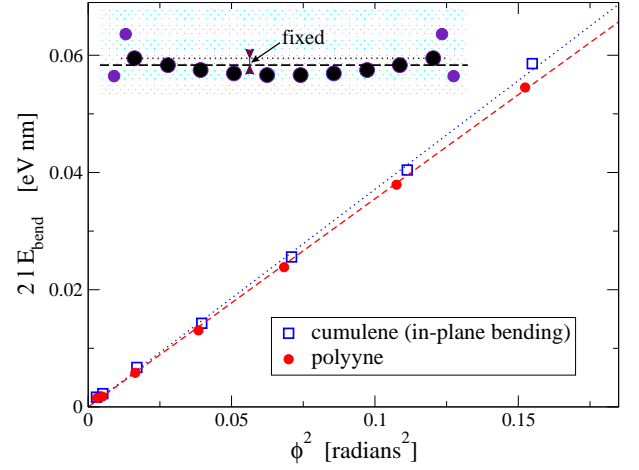


FIG. 3: (Color online) The bending energy $E_{\text{bend}} = E_{\text{mech}} - E_{\text{tens}}$, see Eq. (7), as a function of the squared bending angle of a $\text{-C}_8\text{-}$ chains. Here E_{mech} is the excess energy in the bent configuration induced by the 4-point fixed lateral displacement (at most 30 pm) sketched in Fig. 1, E_{tens} is the value obtained by Eq. (2), using χ as obtained in the straight-chain calculation of Fig. 2. Symbols are the DFT values, lines are linear fits, whose slopes, according to Eq. (4), represent the values of g . Polyynic chain: circles and dashed line; in-plane bent cumulenic chain: squares and dotted line; the out-of-plane bent cumulenic chain results in very similar energies and is not shown for clarity. Inset: an example of fully relaxed in-plane bent configuration of the cumulene $\text{H}_2\text{C-C}_8\text{-CH}_2$.

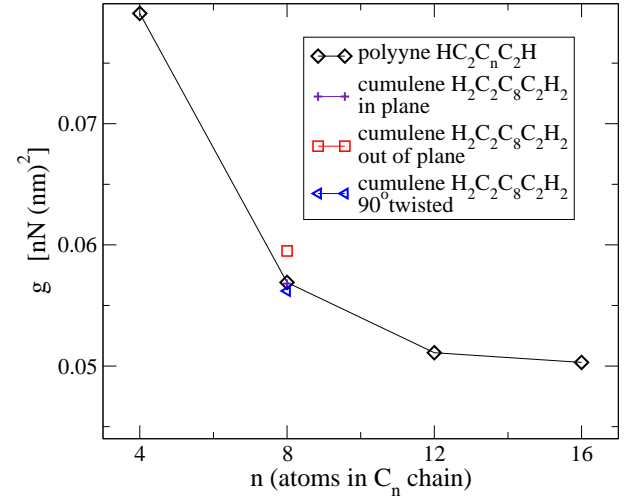


FIG. 4: (Color online) The chain-length dependency of the computed bending stiffness g , as reported in Table I.

are applied at the same time, and deviations extend well outside the linear-response region. In the language of that work, the maximum arc-chord ratio in our calculations is $l/l_s = 1.0064$. We repeat this procedure for several values of the fixed lateral displacements. With the computed DFT energies and structures, we extract the values of g by fitting the angular dependency of E_{bend} in Eq. (4), see Fig. 3.

	HC ₂ -C ₄ -C ₂ H (polyyne)	HC ₂ -C ₈ -C ₂ H (polyyne)	H ₂ C-C ₈ -CH ₂ (cumulene) (planar)		H ₂ C-C ₈ -CH ₂ (cumulene) (90°-twisted)	HC ₂ -C ₁₂ -C ₂ H (polyyne)	HC ₂ -C ₁₆ -C ₂ H (polyyne)
l_0 (C _n) [pm]	377	886	888		889	1395	1903
ε_{ult}	16.2%	16.3%	17.9%		16.8%	16.4%	16.8%
F_{ult} [nN]	12.7	12.3	14.7		12.7	12.1	12.1
χ [nN]	150	156	151		148	149	148
			out-of-plane	in-plane			
g [nN(nm) ²]	7.91 10 ⁻²	5.69 10 ⁻²	5.68 10 ⁻²	5.95 10 ⁻²	5.62 10 ⁻²	5.11 10 ⁻²	5.03 10 ⁻²
$\varepsilon_{\text{crit}}$	-3.7%	-0.458%	-0.470%	-0.493%	-0.473%	-0.174%	-0.093%
F_{crit} [nN]	5.49	0.715	0.710	0.744	0.702	0.259	0.137

TABLE I: The computed mechanical properties of selected carbynes. The elastic tension χ and bending stiffness g define the elastic response, Eq. (7). The ultimate strain ε_{ult} and tension F_{ult} define the maximum stretching that the beam can stand before it breaks. For a C₈ chain section with both ends pinned (hinged, free to rotate), F_{crit} measures the minimum compressive force (with a corresponding strain $\varepsilon_{\text{crit}} = (l_s^{\text{crit}} - l_0)/l_0$ relative to the reported equilibrium length l_0) that must be applied to induce buckling.

The resulting elasticity parameters χ and g are collected in Table I. Despite the different bonding configuration of polyynes and cumulene, the overall longitudinal elasticity χ values are remarkably similar. The value of χ is compatible with a sound velocity $v_s = (\chi/\mu)^{1/2} \simeq 31.5$ km/s for long-wavelength longitudinal vibrations (μ is the linear mass density). In view of the long-range interactions demonstrated recently¹⁷, the weak dependence of χ on the chain length is remarkable. The bending stiffness g is comparatively more sensitive to the chain length, see also Fig. 4. If this velocity is used to evaluate the highest-frequency Brillouin-zone-boundary phonon in a simplest mass-spring chain, one obtains a frequency $\nu_{\text{BZb}} = v_s/(\pi d_{\text{CC}}) \simeq 79$ THz, i.e. a wave number ~ 2600 cm⁻¹, expectedly slightly above the region of the observed high-frequency Raman and infrared modes emerging as the characteristic spectroscopic signatures of the carbynes.^{12,13,27-29}

The cumulene is anisotropic: one can make it bend either within the molecular plane, as sketched in the inset of Fig. 3, or perpendicularly to it, resulting in differently oriented double bonds³⁰ being perturbed. We find that bending is significantly softer for the out-of-plane distortion than for the in-plane one, with a $\sim 5\%$ anisotropy.

The proposed cosine expression for the strain energy given in Eq. (9) of Ref. 20 is compatible with our Eq. (4) for small curvature (although a small amount of longitudinal strain energy is neglected there). The relation $g \simeq d_{\text{CC}}F_d$ obtained based on the average bond length $d_{\text{CC}} = 129$ pm and orientation-dependent bonding strength $F_d = 2.54$ eV as obtained in Ref. 20 yields $g = 5.26 \cdot 10^{-2}$ nN/(nm)², in good agreement with our result, especially with the C₁₂ chain value. This agreement is even more surprising in view of the extreme deformations introduced in Ref. 20, and indicates that the linear-response coefficient of Eq. (4) extends well outside its validity region, provided that the cosine expression

Eq. (9) of that work is adopted.

According to elementary continuum mechanics,³¹ the critical axial load that a beam can sustain in its straight configuration before the onset of the buckling instability is given by Euler's formula

$$F_{\text{crit}} = \pi^2 \frac{g}{l^2}, \quad (8)$$

corresponding to a critical strain

$$\varepsilon_{\text{crit}} = \frac{l_s^{\text{crit}} - l_0}{l_0} \simeq -\frac{F_{\text{crit}}}{\chi} \simeq -\pi^2 \frac{g}{\chi l_0^2}, \quad (9)$$

for a critical sinusoidal lateral deformation profile. By substituting the computed values for χ and g , we find that the C₈ carbyne sustains a critical strain of nearly -0.5% , under the action of a critical force of approximately 0.7 nN, before buckling, as reported in Table I. The corresponding critical strain and force for cumulene (in the softer out-of-plane direction) are essentially equal. The computed values are relevant when both ends of C₈ are pinned (hinged, free to rotate), while if both ends were frozen, the critical force and strain would be four times larger. Likewise, following Eqs. (8) and (9), F_{crit} decays rapidly with size. For example, for C₁₆, whose length is approximately 2.15 times that of C₈, $F_{\text{crit}} = 0.14$ nN, i.e. approximately 20% of the C₈ value only. Direct calculation done for the C₁₂ polyynes in HC₂-C₁₂-C₂H agrees with this scaling, with a small deviation due mostly to a smaller value of g , relative to the C₈ value (while χ is practically coinciding, see Table I).

IV. DISCUSSION AND CONCLUSION

We find it rather surprising that, despite the presence of in principle softer single bonds, the polyynic chain is essentially as hard to compress as double-bonds-based

cumulene. The same essentially equivalent stiffness of polyyne and cumulene is found against bending deformations, but here the result is less unexpected. Even a maximally twisted cumulene in a high-spin electronic state exhibits very similar mechanical properties, see Table I.

We check the obtained buckling critical point for possible effects of chain discreteness or anharmonicity, by running actual simulations. We compare pairs of DFT simulations at fixed strain: one bound to the linear configuration as in Fig. 2, and one starting off in a slightly curved geometry. In the curved simulations, below the buckling instability, the relaxing chain goes back to straight, and recovers the same energy and outward force that the chain produces on the pinned end atoms as in the straight calculation. In contrast, above the buckling instability, a curved shape stabilizes, with a net decrease in total energy and in the force acting on the pinned end atoms. Crosses in Fig. 2 report the fixed-end excess energy of the polyyne chain when allowed to relax in a buckled geometry. We find that the actual buckling instability occurs very close to the linear-response continuum-model value $\varepsilon_{\text{crit}}$ of Eq. (9). Relaxations near instability are rather delicate, since equilibrium is almost indifferent, providing a manifold of almost-equivalent geometrical configurations which give a hard time to the optimization algorithm.

The present work demonstrates that it is possible to go a long way in describing an immaterially thin object such as a monoatomic carbon chain with the mechanics of bulk construction elements, not unlike it was done for 2D graphene in Refs. 32,33. Eventually, carbyne chains turn out rigid enough that the 886 pm-long free-standing C_8 polyyne can sustain a compressive strain of nearly 0.5% before buckling. On the tensile side, we extend our calculations well outside the linear-response region, to estimate the ultimate tensile strength of car-

bynes. The ultimate tension F_{ult} is computed as the maximum force that the carbyne section produces in sustaining an externally imposed longitudinal strain $\varepsilon_{\text{ult}} > 0$. The result in the 10 nN region agrees with previous determinations^{17,34} (but disagrees significantly with the Tersoff-Brenner-model determination of Ref. 35), and indicates that a single molecular chain could be used as a rope to lift a mass as heavy as one microgram without breaking! If one could pack carbynes with a lateral density of one per $A = 0.2 \times 0.2 \text{ nm}^2$ cross-section, one would obtain a material characterized by a remarkable ultimate tensile strength of the order 300 GPa, comparable to that of carbon nanotubes.³⁶

Despite the remarkable mechanical properties of carbynes, their chemical reactivity makes them unsuitable to many applications in real world mechanical situations, where carbon fiber or carbon nanotubes provide superior stability with comparable mechanical properties. However in clean well-isolated nano-engineered devices one could envisage that the usage of C_n chains as structural or elastic elements may lead to consistent advantages over traditional solutions. For example, the soft bending degree of freedom could be exploited for the construction of sensitive accelerometers. Indeed, according to our evaluation of g , a $0.1 \mu\text{g}$ mass hanging at the end of a 37 nm-long C_{30} chain (with the other end bonded to a fixed substrate) would deflect laterally by as much as 1 nm under an acceleration of 0.01 ms^{-2} , i.e. one thousandth of the Earth gravitational field.

Acknowledgments

We acknowledge useful discussion with G. Onida and L. Ravagnan.

-
- ¹ W. Mohr, J. Stahl, F. Hampel, and J. A. Gladysz, *Chem. Eur. J.* **9**, 3324 (2003).
 - ² X. Zhao, Y. Ando, Y. Liu, M. Jinno, and T. Suzuki, *Phys. Rev. Lett.* **90**, 187401 (2003).
 - ³ Y. Liu, R. O. Jones, X. Zhao, and Y. Ando, *Phys. Rev. B* **68**, 125413 (2003).
 - ⁴ K. Inoue, R. Matsutani, T. Sanada, and K. Kojima, *Carbon* **48**, 4209 (2010).
 - ⁵ C. A. Rice, V. Rudnev, R. Dietsche, and J. P. Maier, *Astron. J.* **140**, 203 (2010).
 - ⁶ H. E. Troiani, M. Miki-Yoshida, G. A. Camacho-Bragado, M. A. L. Marques, A. Rubio, J. A. Ascencio, and M. Jose-Yacamán, *Nano Lett.* **3**, 751 (2003).
 - ⁷ C. Jin, H. Lan, L. Peng, K. Suenaga, and S. Iijima, *Phys. Rev. Lett.* **102**, 205501 (2009).
 - ⁸ A. Chuvilin, J. C. Meyer, G. Algara-Siller, and U. Kaiser, *New J. Phys.* **11**, 083019 (2009).
 - ⁹ G. Moras, L. Pastewka, P. Gumbusch, and M. Moseler, *Tribol. Lett.* **44**, 355 (2011).
 - ¹⁰ G. Moras, L. Pastewka, M. Walter, J. Schnagl, P. Gumbusch, and M. Moseler, *J. Phys. Chem. C* **115**, 24653 (2011).
 - ¹¹ C. S. Casari, A. Li Bassi, L. Ravagnan, F. Siviero, C. Lenardi, P. Piseri, G. Bongiorno, C. E. Bottani, and P. Milani, *Phys. Rev. B* **69**, 075422 (2004).
 - ¹² L. Ravagnan, P. Piseri, M. Bruzzi, S. Miglio, G. Bongiorno, A. Baserga, C. S. Casari, A. Li Bassi, C. Lenardi, Y. Yamaguchi, T. Wakabayashi, C. E. Bottani, and P. Milani, *Phys. Rev. Lett.* **98**, 216103 (2007).
 - ¹³ L. Ravagnan, N. Manini, E. Cinquanta, G. Onida, D. Sangalli, C. Motta, M. Devetta, A. Bordon, P. Piseri, and P. Milani, *Phys. Rev. Lett.* **102**, 245502 (2009).
 - ¹⁴ E. Erdogan, I. Popov, C. G. Rocha, G. Cuniberti, S. Roche, and G. Seifert, *Phys. Rev. B* **83**, 041401 (2011).
 - ¹⁵ I. E. Castelli, N. Ferri, G. Onida, and N. Manini, *J. Phys.: Condens. Matter* **24**, 104019 (2012).
 - ¹⁶ E. Hobi Jr., R. B. Pontes, A. Fazzio, and A. J. R. da Silva, *Phys. Rev. B* **81**, 201406 (2010).
 - ¹⁷ S. Cahangirov, M. Topsakal, and S. Ciraci, *Phys. Rev. B*

- 82**, 195444 (2010).
- ¹⁸ M. Topsakal and S. Ciraci, Phys. Rev. B **81**, 024107 (2010).
 - ¹⁹ B. Akdim and R. Pachter, ACSNano **5**, 1769 (2011).
 - ²⁰ Y. H. Hu, J. Phys. Chem. C **115**, 1843 (2011).
 - ²¹ C. Ataca and S. Ciraci, Phys. Rev. B **83**, 235417 (2011).
 - ²² A. D. Becke, J. Chem. Phys. **98**, 5648 (1993).
 - ²³ J. P. Perdew, K. Burke, and M. Ernzerhof, Phys. Rev. Lett. **77**, 3865 (1996).
 - ²⁴ X. Xu and W. A. Goddard III, J. Chem. Phys. **121**, 4068 (2004).
 - ²⁵ P. Giannozzi, S. Baroni, N. Bonini, M. Calandra, R. Car, C. Cavazzoni, D. Ceresoli, G. L. Chiarotti, M. Cococcioni, I. Dabo, A. Dal Corso, S. de Gironcoli, S. Fabris, G. Fratesi, R. Gebauer, U. Gerstmann, C. Gougousis, A. Kokalj, M. Lazzeri, L. Martin-Samos, N. Marzari, F. Mauri, R. Mazzarello, S. Paolini, A. Pasquarello, L. Paulatto, C. Sbraccia, S. Scandolo, G. Sciauzero, A. P. Seitsonen, A. Smogunov, P. Umari, and R. M. Wentzcovitch, J. Phys.: Condens. Matter **21**, 395502 (2009), <http://www.quantum-espresso.org>.
 - ²⁶ W. A. Chalifoux and R. R. Tykwinski, C. R. Chimie **12**, 341 (2009).
 - ²⁷ F. Cataldo, L. Ravagnan, E. Cinquanta, I. E. Castelli, N. Manini, G. Onida, and P. Milani, J. Phys. Chem. B **114**, 14834 (2010).
 - ²⁸ L. Ravagnan, E. Cinquanta, D. Sangalli, and P. Milani, Phys. Status Solidi B **247**, 2017 (2010).
 - ²⁹ F. Innocenti, A. Milani, and C. Castiglioni, J. Raman Spectrosc. **41**, 226 (2010).
 - ³⁰ N. Manini and G. Onida, Phys. Rev. B **81**, 127401 (2010).
 - ³¹ S. P. Timoshenko and J. M. Gere, *Theory of Elastic Stability*, 2 ed. (McGraw-Hill, New York, 1961).
 - ³² E. Cadelano, P. L. Palla, S. Giordano, and L. Colombo, Phys. Rev. Lett. **102**, 235502 (2009).
 - ³³ E. Cadelano, S. Giordano, and L. Colombo, Phys. Rev. B **81**, 144105 (2010).
 - ³⁴ T. I. Mazilova, S. Kotrechko, E. V. Sadanov, V. A. Ksenofontov, and I. M. Mikhailovskij, Int. J. Nanoscience **9**, 151 (2010).
 - ³⁵ T. Ragab and C. Basaran, J. Electr. Packaging **133**, 020903 (2011).
 - ³⁶ M.-F. Yu, O. Lourie, M. J. Dyer, K. Moloni, T. F. Kelly, and R. S. Ruoff, Science **287**, 637 (2000).
 - ³⁷ D. Vanderbilt, Phys. Rev. B **41**, 7892 (1990).
 - ³⁸ F. Favot and A. Dal Corso, Phys. Rev. B **60**, 11427 (1999).
 - ³⁹ To compute reliable small energy differences, we impose severe self-consistency requirements: we accept the electronic-structure self consistency when the total adiabatic energy is converged to better than 10^{-10} Ry $\simeq 1$ peV, and push atomic coordinates relaxation until all force components are smaller than 10^{-5} Ry/ $a_0 \simeq 0.4$ pN. We use ultrasoft pseudopotentials,^{37,38} for which a moderate cut-off for the wave function/charge density of 30/240 Ry is sufficient. To address isolated molecules in the repeated-cell geometry implied by plane waves, we make sure that at least 1 nm of vacuum separates all atoms in adjacent periodic images.
 - ⁴⁰ We fit the value of d by minimizing the squared distance of the relaxed atomic positions in the $x-z$ plane from the circular arc $x = d - r + (r^2 - z^2)^{1/2}$, whose radius $r = (l_s^2 + 4d^2)/(8d)$ is determined by taking into account the separation l_s of the terminal atoms of the C₈ chain section, namely those kept at $x = 0$.